



## CFD AND EXPERIMENTAL ANALYSIS ON THERMAL PERFORMANCE OF EXHAUST SYSTEM OF A SPARK IGNITION ENGINE

Mesut DURAT\*, Zekeriya PARLAK\*\*, Murat KAPSIZ\*\*\*, Adnan PARLAK\*\*\*\* ve Ferit FIÇICI\*

\*Sakarya University Technical Education Faculty, Department of Mechanical Education, 54188, Sakarya, durat@sakarya.edu.tr, fficici@sakarya.edu.tr

\*\*Sakarya University, Faculty of Engineering, Department of Mechanical Engineering 54187, Sakarya, zparlak@sakarya.edu.tr

\*\*\*Sakarya University, Technology Faculty, Department of Mechanical Engineering 54188, Sakarya, mkapsiz@sakarya.edu.tr

\*\*\*\*Yıldız Technical University, Naval Architect and Marine Engineering Faculty 34349, Istanbul, aparlak@yildiz.edu.tr

(Geliş Tarihi :28.09.2011 Kabul Tarihi:20.06.2012)

**Abstract:** Catalysts of a gasoline engine become active when the exhaust temperature exceeds 200 °C. Cold start HCs are extremely high until catalysts reach the light-off temperature. Determination of optimum place and necessary time of the catalyst to reach this temperature is of vital importance. Interaction between exhaust gas and inner wall, along with the exhaust pipe needs to be well-understood. The interaction can be computed by numerical solutions based on fluid dynamics and heat transfer equations depending on time and location. In the study, three-dimensional transient CFD analysis has been performed for the whole exhaust pipe. The results of CFD analysis was in very good agreement with those of experimental data. Also, an optimal catalyst location was determined by the CFD analysis performed in transient regime. Heat transfer phenomena were also investigated analytically using different Nusselt number correlations given in the literature. Analytic results were compared with those of the experimental data. Each correlation gave reasonable results with different range of Reynolds number.

**Keywords:** Exhaust Pipe, Catalyst, Computational Fluid Dynamics, CFD, Heat Transfer Analysis

## BİR BUJİ ATEŞLEMELİ MOTORUN EGZOZ SİSTEMİNİN TERMAL PERFORMASININ CFD VE DENEYSEL ANALİZİ

**Özet:** Benzinli bir motorların katalitik dönüştürücüleri egzoz sıcaklığı 200 °C'yi aştığında devreye girer.. İlk çalıştırmada HC değerleri katalitik dönüştürücü bu sıcaklığa ulaşana kadar önemli oranda yüksek olacaktır. katalitik dönüştürücünün bu sıcaklığa erişmesi gerekli olan optimum konum ve zaman hayati bir öneme sahiptir. Egzoz gazı ve egzoz borusunun iç duvarı arasındaki etkileşimin iyi anlaşılması gerekmektedir. Bu etkileşim akışkanlar dinamiği ve ısı transferi denklemleri temelinde zamana ve konuma bağlı olarak numerik olarak hesaplanabilmektedir. Bu çalışmada üç boyutlu zamana bağlı bir CFD analizi tüm egzoz borusu için gerçekleştirildi. CFD analizi sonuçları aynı egzoz için yapılan deneysel verilerle iyi bir uyum gösterdi. Aynı zamanda bir optimal katalitik dönüştürücü konumu gerçekleştirilen bu zamana bağlı CFD analizi ile belirlendi. Isı transferi olayı da literatürde verilen Nusselt sayısı bağlantıları kullanılarak analitik olarak araştırıldı. Analitik sonuçlar deneysel verilerle karşılaştırıldı ve her bir bağıntı Reynolds sayılarının farklı aralıkları ile uyumlu olacak şekilde sonuçlar verdi.

**Anahtar kelimeler:** Egzoz borusu, Katalitik Dönüştürücü, Hesaplamalı Akışkanlar Dinamiği, CFD, Isı Transferi Analizi

### NOMENCLATURE

$c_p$	Specific heat capacity, $m^2 s^{-2} K^{-1}$	$A$	Cross-section area, $m^2$
$\dot{m}$	mass flow rate, $kg s^{-1}$	$D$	Hydraulic diameter, m
$S_E$	Energy source, $kg m^{-1} s^{-3}$	$L$	entrance length, m
$S_M$	Momentum source, $kg m^{-2} s^{-2}$	$Nu$	Nusselt Number
$\Delta T_{lm}$	logarithmic temperature difference	$T$	Temperature, K
$h$	Enthalpy, $m^2 s^{-2}$	$d$	pipe inside diameter, m
$Pr$	Prandtl number	$f$	friction factor
$Re$	Reynolds Number	$k$	Turbulence kinetic energy, $m^2 s^{-2}$
		$p$	Pressure, Pa
		$\dot{Q}$	Heat rate, $kg m^2 s^{-3}$

$t$	Time, s
$u$	Fluctuating velocity component, $\text{m s}^{-1}$
$U$	Averaged velocity component, $\text{m s}^{-1}$

#### **Greek Symbol**

$\rho$	Density, $\text{kg m}^{-3}$
$\alpha_1$	Cosntant, 5/9
$\lambda$	thermal conductivity, $\text{kg m s}^{-3}\text{K}^{-1}$
$\mu$	Viscosity, $\text{kg m}^{-1}\text{s}^{-1}$
$\tau$	molecular stress tensor, $\text{kg m}^{-1}\text{s}^{-2}$

#### **Subscript**

s	solid
g	gas
t	turbulent
tot	total

## **INTRODUCTION**

The development of power units with low environmental impact has become one of the most interesting challenges in the automotive technology. From the perspective of environmental protection, researchers must further decrease exhaust emissions of gasoline engines for automobiles. Many efforts are being made to reduce air pollution from automotive engine emissions. Standards, which are developed to control the different undesirable species, are becoming more stringent requiring the reduction of engine out emissions, as well as the use of after-treatment systems in the exhaust system (Henein and Tagomori, 1999). Catalysts have become so effective in the last 15 years that it is even becoming difficult to measure the regulated pollutants, i.e. CO, HC and  $\text{NO}_x$ , when the catalyst has reached its light-off temperature (Favez et al., 2009). To succeed this, it is extremely important to reduce emissions of harmful components, especially the unburned HC from the engine during the start/ warm-up process which involves inadequate catalytic activity (Hattori et al., 1997). The effectiveness of these converters depends on the exhaust gas temperature, which is fairly low during cold-start (Gallopoulos, 1992; Boam et al., 1995). Since catalysts are effective only at high temperature, emissions are far more significant during the initial part (cold phase) of a trip when engine and catalyst are cold (Favez et al., 2009). Thus, detailed analysis is required to shorten the time necessary which the catalytic converter reaches the light-off temperature.

Baba et al. (1996) used a 2-D simulation model to search the effects of the loading quantity of the noble metals for improved catalyst conversion efficiency. Yaegashi et al. (1994) applied the simulation technique to optimize the heating pattern of an electrically heated catalyst. Koltsakis et al. (1997) developed a 2-D model for Three Way Catalyst (TWC) to study the effects of running conditions on the catalyst performance. Chan and Hoang (1999) considered the real engine cold-start conditions where the wall temperatures of the exhaust system and the catalytic converter are gradually heated up by the exhaust gas.

Many authors have dealt with analytical solutions of the heat transfer in exhaust systems. Depcik and Assanis (2002) examined Nusselt numbers which have different formulations in literature depending on Reynolds number. Caton and Heywood (1981) developed and experimentally verified their models for the instantaneous heat transfer in an engine exhaust port.

The heat transfer analysis was presented at many works as steady and transient states. Kandylas and Stamatelos (1999) presented experimental data from steady state and transient heat transfer measurements, they analyzed a transient computer model on all exhaust pipes and results of the analysis were compared to experimental data. Sorin et al. (2008) presented a study estimating the instantaneous character of heat transfer coefficient in exhaust pipes for the continuous and intermittent flows. The authors concluded that, transient solution of the heat transfer equations was necessary to find out the instantaneous character of heat transfer coefficient.

Many studies have been presented considering transient and steady-state modes numerically related to the heat transfer and fluid flow throughout the exhaust systems. Among them, Silva et al. (2006) developed a mathematical model based on energy and mass balance equation, which are obtained for exhaust gas and pipe wall separately, for catalytic converter and solved the equations numerically by dividing the catalytic converter into certain number of longitudinal elements as steady state.

An exhaust gas system has to satisfy the thermodynamic efficiency along with architectural and environmental impact, noise levels, structural resistance, etc. In order to properly take into account all these features, the use of multidisciplinary tools (CAD solid modeling, FEM and CFD analysis, etc.) has begun to be also used for the design of the exhaust gas systems (Pinelli and Bucci, 2009). To realize the heat and fluid flow processes at different time and location in exhaust pipe, numerical flow simulations (computational fluid dynamics-CFD) are required. CFD provide both visually and numerically results in three dimensions as transient solution. Additionally, a commercial CFD code eliminates the difficulty of complex numeric solutions.

A catalyst of a gasoline engine becomes active when the exhaust temperature is above  $200\text{ }^\circ\text{C}$  (the light-off temperature). Cold start HCs are extremely high until catalyst reaches this temperature. Thus, determination of the optimum place and the time which the catalyst reaches this temperature is important. For this reason, interaction between exhaust gas and inner wall along with the exhaust pipe needs to be well-known. The interaction can be computed by numerical solutions based on fluid dynamics and heat transfer equations depending on time and location. The main contribution of the study is that optimal location of catalyst of a gasoline engine is to specified after reaching the light-off temperature at any location of exhaust pipe as early

as possible by using CFD analysis confirmed by experimental data.

In the present study, three dimensional transient CFD analyses have been performed for the whole the exhaust pipe. Results of CFD analysis have been compared with those of experimental study for various time steps. Moreover, heat transfer phenomena has also been investigated analytically in the paper by using equations given in the literature. The values of Nusselt number have been obtained using experimental data and compared with results of the equations.

## EXPERIMENTAL APPARATUS and PROCEDURES

Water cooled four cylinders Fiat engine was instrumented for the detailed measurement of the different operating parameters during the first few minutes of engine start-up. The exhaust system of the engine was equipped with a TWC under investigation. The exhaust system consists of three distinct parts, which includes an exhaust manifold, an exhaust pipe and a catalytic converter. The measurements included manifold outlet exhaust gas temperature, catalytic converter inlet exhaust gas temperature and engine speed. Thermocouples were embedded in two locations, on exhaust manifold outlet and on catalytic converter inlet, for temperature control. The test engine specifications are shown in Table 1.

**Table 1.** Test engine specifications

Engine Type	4 Cylinders Water Cooled Engine
Displacement	1580 cc
Bore x Stroke	86 x 67 mm
Compression ratio	9.2:1
Maximum Power	86 HP / 5800 rpm
Maximum Torque	13.5 kgm / 2900 rpm

Elimko K type thermocouples are made of NiCr-Ni material in accordance with DIN 43710 standard. Temperature data were collected by Agilent 34970A modeling data logger apparatus. These data were then transferred to a personal computer for analysis. The experimental set up used in the study is shown in the Figure 1.

The engine was operated at idle condition and at the speed of  $1200 \pm 20$  rpm. Experimental study was conducted at the environmental temperature of  $25 \text{ }^\circ\text{C}$  and at the idle condition engine for the first 125 s after the engine is started. The temperature measurements were made both from inlet and outlet points of catalytic converter. The measurements were repeated 5 times to minimize the measuring uncertainties.

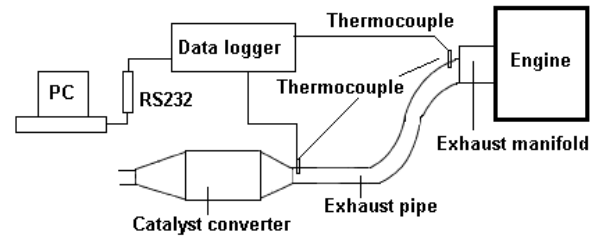


**Figure 1.** Schematic layout of exhaust system on engine

## CFD ANALYSIS

Analytical solutions to the Navier-Stokes equations exist for only the simplest of flows under ideal conditions. To obtain solutions for real flows, a numerical approach must be adopted whereby the equations are replaced by algebraic approximations that can be solved using a numerical method (ANSYS, 2010). CFD is a numerical method that can be solved real fluid flow. In the presented study, CFD analysis of the exhaust pipe was performed with CFX in ANSYS Workbench V12.1 with three dimensional CFD numerical codes.

### CFD Mesh

Solid pipe and fluid volume in the exhaust pipe are specified as computational domain. The ANSYS fluid flow tool (CFX) generates mesh automatically using CAD model. The algorithm generates the mesh based on the geometry increasing the number of cells in proximity of wall of the pipe. Hence, boundary layer profile which is important for determining where turbulence flow starts can correctly be predicted by the grid intensity near the wall. In the paper; as can be seen in Fig 2., the exhaust pipe used in the CFD analysis has been divided into 103148 tetrahedral elements and 42578 nodes for mesh generation.

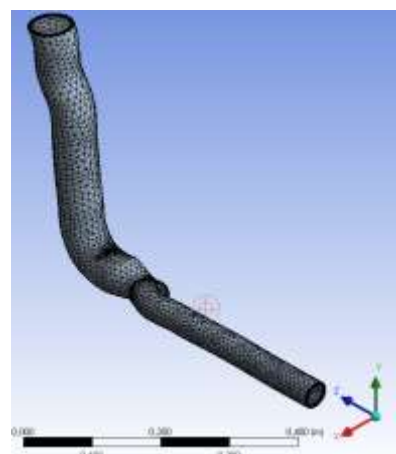


**Figure 2.** Mesh of the exhaust pipe CFD Model

The CFX code solves Navier-Stokes equations using a finite volume method for the equation discretization. Heat transfer in a fluid domain is governed by the thermal energy equation on CFX (Eq. 1). Since viscous

heating is considered as significant viscous dissipation term was included in the energy equation.

$$\frac{\partial(\rho h)}{\partial t} - \frac{\partial p}{\partial t} + \nabla \cdot (\rho \mathbf{U} h) = \nabla \cdot (\lambda \nabla T) + \mathbf{U} \cdot \nabla p + \tau : \nabla \mathbf{U} + S_E \quad (1)$$

The term  $\tau : \nabla \mathbf{U}$  is always positive and called viscous dissipation and  $\tau$  is the molecular stress tensor (including both normal and shear components of the stress) (ANSYS, 2010).

Shear Stress Transport (SST) turbulence model was used in the work. This is a good choice because it accounts for the transport of the turbulent shear stress and gives highly accurate predictions of the onset and the amount of flow separation (ANSYS, 2009).

The SST model is considered the best model because it does the best overall job in predicting the complex flows involving separation while giving results comparable with the best of the other models. With regard to the numerical performance, SST model gives good result (Bardina et al., 1997). The Navier-Stokes equations describe both laminar and turbulent flows without the need for additional information.

In general, turbulence models seek to modify the original unsteady Navier-Stokes equations by the introduction of averaged and fluctuating quantities to produce the Reynolds Averaged Navier-Stokes (RANS) equations (ANSYS, 2010). These equations represent the mean flow quantities only, while modeling turbulence effects without a need for the resolution of the turbulent fluctuations. Turbulence models based on the RANS equations are known as Statistical Turbulence Models due to the statistical averaging procedure employed to obtain the equations (ANSYS, 2010). The averaging procedure introduces additional unknown terms containing products of the fluctuating quantities, which act like additional stresses in the fluid. These terms, called ‘‘turbulent’’ or ‘‘Reynolds’’ stresses, are difficult to determine directly and so become further unknowns. The Reynolds (turbulent) stresses need to be modeled by a sufficient number of equations for all the unknowns. Reynolds Averaged Navier-Stokes (RANS) transport equation is:

$$\frac{\partial p}{\partial t} + \frac{\partial}{\partial x_j} (\rho U_j) = 0 \quad (2)$$

$$\frac{\partial \rho U_i}{\partial t} + \frac{\partial}{\partial x_j} (\rho U_i U_j) = -\frac{\partial p}{\partial x_i} + \frac{\partial}{\partial x_j} (\tau_{ij} - \rho \overline{u_i u_j}) + S_M \quad (3)$$

where  $\tau$  he molecular stress tensor. The continuity equation has not been altered but the momentum and

scalar transport equations contain turbulent flux terms additional to the molecular diffusive fluxes. These are the Reynolds stresses,  $\rho \overline{u_i u_j}$  (ANSYS, 2010)..

$$-\rho \overline{u_i u_j} = \mu_t \left( \frac{\partial U_i}{\partial x_j} + \frac{\partial U_j}{\partial x_i} \right) - \frac{2}{3} \delta_{ij} \left( \rho k + \mu_t \frac{\partial U_k}{\partial x_k} \right) \quad (4)$$

where  $\mu_t$  is the eddy viscosity or turbulent viscosity, which must be modeled. RANS energy equation is:

$$\frac{\partial \rho h_{tot}}{\partial t} - \frac{\partial p}{\partial t} + \frac{\partial}{\partial t} (\rho U_j h_{tot}) = \frac{\partial}{\partial x_j} \left( \lambda \frac{\partial T}{\partial x_j} - \rho \overline{u_j h} \right) + \frac{\partial}{\partial x_j} [U_i (\tau_{ij} - \rho \overline{u_i u_j})] + S_E \quad (5)$$

where  $h_{tot}$  is total enthalpy is given by:

$$h_{tot} = h + \frac{1}{2} U_i^2 + k \quad (6)$$

where  $k$  is turbulent kinetic energy,  $k = \frac{1}{2} \overline{u_i^2}$ . Reynolds Averaged Navier-Stokes (RANS) energy equation contains an additional turbulence flux term,  $\rho \overline{u_j h}$  which is equal to  $\frac{\mu_t}{Pr_t} \frac{\partial h}{\partial x_j}$ ,  $Pr_t$  is the turbulent Prandtl number. The  $\frac{\partial}{\partial x_j} [U_i (\tau_{ij} - \rho \overline{u_i u_j})]$  term in the equation is the viscous work term. The proper transport behavior for the SST model can be obtained by a limiter to the formulation of the eddy-viscosity:

$$v_t = \frac{\alpha_1 k}{\max(\alpha_1 \omega, S F_2)} \quad (7)$$

where  $v_t = \frac{\mu_t}{\rho}$ .

Again  $F_2$  is a blending function that restricts the limiter to the wall boundary layer.  $\alpha_1 = 5/9$  and  $S$  is an invariant measure of the strain rate.  $\omega$  is turbulent frequency (ANSYS, 2010).

ANSYS CFX enables to create solid domains in which the equations for heat transfer are solved. This is known as conjugate heat transfer as given (ANSYS, 2010):

$$\frac{\partial(\rho h)}{\partial t} + \nabla(\rho U_s h) = \nabla(\lambda_s \nabla T) + S_E \quad (8)$$

where  $\lambda_s$  is thermal conductivity of the solid.  $U_s$  is the solid velocity, if specified, and  $S_E$  is an optional volumetric heat source.

These equations are solved over each control volume in the flow domain using numerical solution. The numerical algorithm is to discrete the equations.

Transient simulation which is solved by computing a solution for many discrete points in time was realized at the CFD analysis. Time dependent behavior is specified through time step which provides a way to track the progress of real time during the simulation. Time step was set to  $t=1$  s and total simulation time was specified as 129 s in parallel with experimental work.

### Boundary Conditions

A coupled solution is carried out including the pipe as solid domain in the analysis. Conjugate heat transfer model is implemented in ANSYS CFX for the solid domain. In the analysis there are four boundary conditions, consisting of inlet, outlet, inside wall and outside wall of the pipe (Figure 3). The boundary conditions are constructed with mass flow rate and temperature at inlet, static pressure at outlet and temperature at wall. The inside wall is defined as domain interface which is assigned fluid-solid interaction. The mass flow, temperature, static pressure values were obtained by experiments

The mass flow rate at inlet was set to  $\dot{m} = 0.011$  kg/s . The value stays constant during the simulation. Because the temperature measured at inlet varied depending on time, the value was set as a time-dependent equation on CFX (Eq. 9).

$$T_{g,inlet} = 1.5 t + 359.3 \quad (9)$$

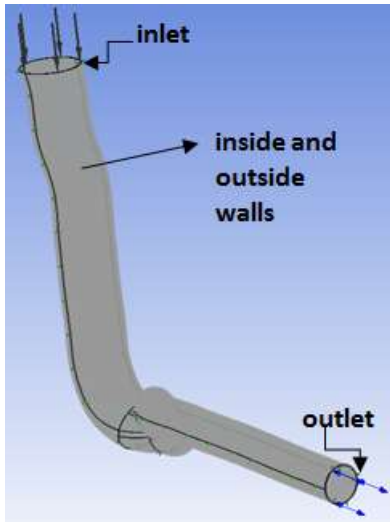


**Figure 3.** Boundaries of the exhaust pipe  
The outlet was specified as opening boundary condition that allows the fluid to cross the boundary surface in either direction. An opening boundary condition might be used where it is known that the fluid flows in both directions across the boundary (ANSYS, 2010). The outlet pressure measured equals to 1.1 bar and the value was set on CFX. The opening temperature was set to the temperature value calculated at the previous time step. In this paper, it is considered that the wall temperature is constant and investigated for the constant wall temperature boundary condition of the solid domain. Numerous experimental investigations of heat transfer

are conducted under conditions of either constant surface heat flux or of constant wall temperature (Buznik et al., 1966; Bagheri et al., 1995; Hua et al., 2007, Marineau et al., 2007; Abarhama et al., 2010). Therefore the wall temperature was fixed to 293 K in the study.

### PROPERTIES OF EXHAUST GAS

The properties of the exhaust gas have been calculated form (Boam et al., 1995):

$$\rho = \frac{353}{T_g} \quad (10)$$

$$c_p = 962.097 + 0.1507T_g \quad (11)$$

$$\lambda = 8.459 \times 10^{-3} + 5.7 \times 10^{-5}T_g \quad (12)$$

$$\mu = 1.384 \times 10^{-5} + 2.68 \times 10^{-8}T_g \quad (13)$$

where  $\rho$  is the exhaust gas density,  $c_p$  is heat capacity of the exhaust gas,  $T_g$  is the exhaust gas temperature,  $\lambda$  is thermal conductivity and  $\mu$  is dynamic viscosity of the exhaust gas. The equations were written as expressions individually and the exhaust gas material was inserted using the equations in material properties on CFX.

### HEAT TRANSFER IN THE EXHAUST PIPE

One of aims of the study was to investigate heat transfer between exhaust gas and pipe wall. Influence of the heat transfer phenomena also gets a better understanding analytically along with CFD analysis. In addition, heat transfer coefficients varying in time can be obtained by evaluating experimental data.

Parameters which are involved in the computational modeling of the heat transfer in exhaust system are reviewed. The relations and laws of heat transfer presented different equations are calculated accordingly. The flow in the exhaust pipe is unsteady and compressible. The flow condition at any location and time of interest helps to describe heat transfer. The heat transfer from the exhaust gas to the inner wall of the exhaust pipe is mainly due to forced convection and is strongly dependent on the exhaust flow characteristic and geometry of the pipe. Heat energy balance is expressed as (Chan and Hoang, 1999):

$$\dot{Q} = \dot{m}c_p(T_i - T_o) \quad (14)$$

where  $T_i$  is inlet temperature and  $T_o$  is outlet temperature.

The heat transfer coefficient value estimated in time is compared to the heat transfer coefficient value measured. The heat transfer coefficient:

$$h_g = \frac{\dot{Q}}{A_s \Delta T_{lm}} \quad (15)$$

where  $\Delta T_{lm}$  is the logarithmic temperature difference and expressed as follows:

$$\Delta T_{lm} = \frac{\Delta T_i - \Delta T_o}{\ln \left( \frac{\Delta T_i}{\Delta T_o} \right)} \quad (16)$$

In this expressions  $\Delta T_i$  and  $\Delta T_o$  is difference between the gas and wall temperature at pipe inlet and outlet, respectively. The estimation of heat transfer rates is not very sensitive in the values of pipe wall temperatures (Kandylas and Stamatelos, 1999). In the study, the calculations of heat transfer were carried out according to constant surface temperature. The Nusselt number value allows appreciating the flow role and is described as follows:

$$Nu = \frac{h_g D}{\lambda} \quad (17)$$

where  $D$  is the hydraulic diameter. A number of Nusselt number correlations have been developed to describe the heat transfer in turbulent pipe flow. Nusselt correlations can be expressed as follows:

$$Nu = c Re^a Pr^b \quad (18)$$

$a$ ,  $b$  and  $c$  coefficients, which can be obtained experimentally, vary depending on some factors such as temperature, fluid type, geometrical dimensional.  $Re$  and  $Pr$  are Reynolds number and Prandtl number and expressed as  $Re = \frac{\rho U D}{\mu}$  and  $Pr = \frac{c_p \mu}{\lambda}$ , respectively. In the study, experimental data which is provided by measurement of temperature and mass flow was compared to those values obtained by some correlations in the literature. One of the first equations developed is Dittus-Boelter equation:

$$Nu = 0.023 Re^{0.8} Pr^{1/3} \quad (19)$$

The Nusselt number related to Prandtl number and Reynolds number. The typical flow conditions in automotive exhaust systems produce  $Re$  numbers in the range that the flow remains turbulent (Kandylas and Stamatelos, 1999). Eq. (19) is used for fully developed turbulent flow in a smooth circular tube and for  $Re > 10000$  (Caton and Heywood, 1981). For the flow characterized by large property variations, a correlation determined by Seider-Tate is used:

$$Nu = 0.027 Re^{0.8} Pr^{1/3} \left( \frac{\mu}{\mu_{su}} \right)^{0.14} \quad (20)$$

where  $\mu$  and  $\mu_{su}$  are viscosities at bulk and surface temperatures, respectively. Eq. (20) is used for fully developed turbulent flow in a smooth circular tube and for  $Re > 10000$  and  $0.7 < Pr < 16700$ . In order to account for effect of wall roughness, Gnielinski included the friction factor  $f$  as follows:

$$Nu = \frac{(f/8)(Re - 1000)Pr}{1.07 + 12.7\sqrt{(f/8)}(Pr^{2/3} - 1)} \quad (21)$$

$$f = \frac{1}{(1.58 \ln Re - 3.28)^2} \quad (22)$$

Eq. (21) is used for fully developed turbulent flow in a smooth circular tube in the cases of  $10^4 > Re > 10^6$  and  $0.5 < Pr < 2000$ .

The heat transfer coefficient measured in takedown section of an exhaust systems by Sachdev and Sorenson (1981) were correlated by Meisner and Soreson (1986) to yield the following relation:

$$Nu = 0.0774 Re^{0.769} \quad (23)$$

The equation could be accurately in the range  $10^3 > Re > 10^4$  (Kandylas, and Stamatelos, 1999). Petukhov (1970) suggested a correlation for fully developed turbulent and transition flow and  $Re > 2300$ ;

$$Nu = \frac{\xi}{8} (Re - 1000) Pr \left[ 1 + \left( \frac{D}{L} \right)^{2/3} \right] \quad (24)$$

$$\xi = \frac{1}{(1.82 \log(Re) - 1.64)^2} \quad (25)$$

The correlation is valid with  $Pr > 0.7$ . Shayler et al. (1995) corrected experimental data by Eq. (26)

$$Nu = 0.14 Re^{0.68} \quad (26)$$

Wendland (1993) suggest to use a correlation coefficient on the Sieder-Tate equation:

$$Nu = 0.027 Re^{0.8} Pr^{1/3} \left( \frac{\mu}{\mu_s} \right)^{0.14} C_{entr} \quad (27)$$

$C_{entr}$  is account for separation effect of the fluid from wall when it initially enters the pipe Sachdev and Sorenson (1981).

$$C_{entr} = 0.892 + \frac{2.02}{L/d} \quad (28)$$

where  $d$  is the pipe inside diameter and  $L$  is the entrance length. Depcik and Assanis (2002) proposed a universal, quasi-steady correlation that cloud be used to determine the heat transfer in the intake or exhaust of an internal combustion engine:

$$Nu = 0.07 Re^{3/4} \quad (29)$$

## RESULTS AND DISCUSSIONS

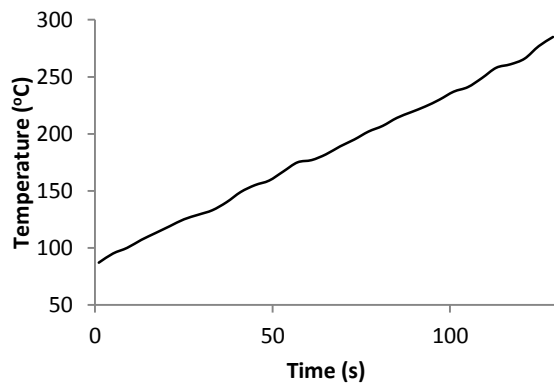
### Results of CFD Analysis

Experiments and CFD analysis were carried out for an average mass flow rate of 0.011 kg/s The total time was set to 129 s and the time step for CFD analysis was set to 1s. The gas density, heat capacity, thermal conductivity and dynamic viscosity of the exhaust gas were calculated from Eq. (10) to Eq. (13) for CFD analysis. Because the exhaust gas was defined as a real

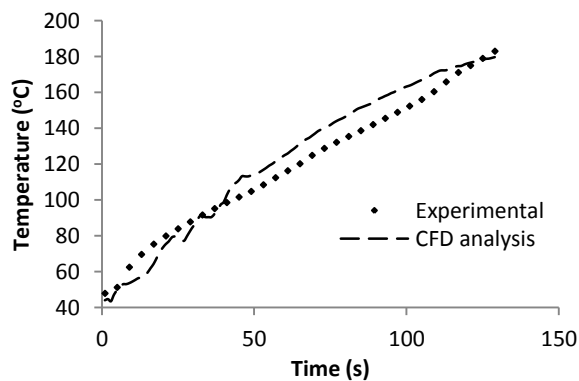
gas in CFX, compressible fluid models were used in the analysis (ANSYS, 2010).

Figure 4 shows the variation of temperatures depending on time, which was measured at the exhaust manifold outlet. The thermocouple used for measuring temperature has been placed at a distance of 0.75 mm from inner surface of the exhaust pipe wall.

Figure 5 shows the comparison of exhaust temperatures calculated by CFD analysis at the catalyst inlet with the experimental data. The temperature of the outlet was measured with thermocouples which were set at a distance of 0.75 mm from inner surface and the value was taken at the same point in CFD analysis for comparison between experimental data and CFD results (Figure 6). As it is seen in Figure 5, the results obtained by CFD analysis showed fairly good agreement with the experimental results. The results of the analysis clearly reveal that there is good agreement until 40s corresponding to about  $Re > 12 \times 10^3$ . The Results which are between 40s and 120s corresponding to  $10 \times 10^3 < Re < 12 \times 10^3$  have a small deviation from the experimental data. The CFD results showed an exponential form after 120th seconds while the experimental results showed a linear form.



**Figure 4.** Temperatures measured at the inlet of the exhaust pipe



**Figure 5.** Comparison to transient measurements and CFD results

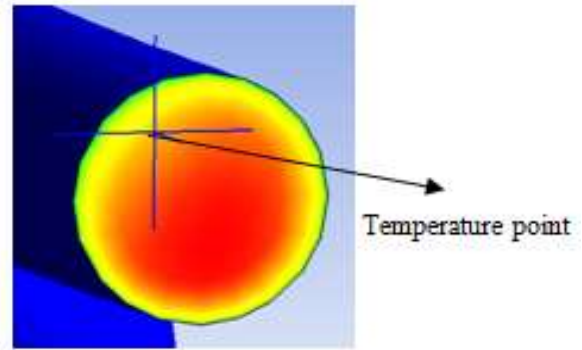


**Figure 6.** Outlet temperature point of CFD analysis

In Figure 7, it can be seen that velocity streamlines at 73s. The velocity values vary between 5.78 m/s and 0.92 m/s. During the gas flow to the outlet, the velocity increased as expected because of the reduction in cross-section. The velocity which is about 1.66 m/s at inlet becomes 5.78 m/s in some regions especially at elbow towards the outlet of the pipe.

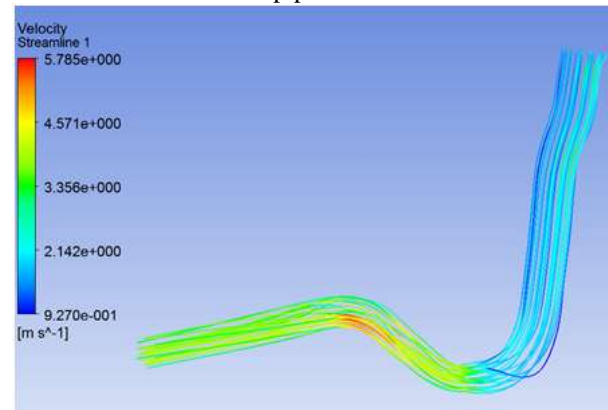


**Figure 7.** Velocity streamline at 73s

In Figure 8, it can be seen that there is a temperature variation on a plane at 123s. The minimum temperature on the plane is 298 K and is on pipe wall. As can be seen from Figure 8, in the inlet section of the pipe the temperature stays at high values and then decreases. The region which has higher velocity at the last elbow towards the outlet of the pipe, as mentioned previously, has higher temperature than the other regions on same cross-section. The region near the wall stays always in low temperature values due to the constant wall temperature. Cooling can be seen well in Figure 9 by the help of temperature contours for inlet and outlet pipe. The temperature profile on a line of a plane at 0.16 m at 120s can be seen in Figure 10. It is observed from the CFD analysis that the temperature stays high at especially pipe core for all cross-section of the pipe and the temperature distribution is generally regular.

From the CFD analysis, temperature of inside wall, which is on interaction of solid and gas, was represented on Figure 11. Wall heat flux for inside wall of the exhaust pipe can be estimated as can be seen Figure 12. As expected, heat flux increases in the time because temperature of inlet increases in the time. Value of the heat flux is about 6 kW/m<sup>2</sup> at 129 s. Figure 13 shows wall heat transfer coefficient for inside wall of the

exhaust pipe from CFD analysis. This values imply a strong heat influence on the exhaust pipe.

Determination of the optimal location of the catalyst along with the exhaust pipe is important. If the time which the catalyst reaches the light-off temperature is shortened, HC emissions during cold start will be further minimized. Figure 14. shows temperature profiles along with the exhaust pipe for various times. The figure shows that the catalyst doesn't reach the light-off temperature before 76 s. The light-off temperature is possible for 77 s, if the catalyst is located closer than 0.23 m to the manifold outlet. The figure also shows that if the catalyst is located closer than 0.3 m to the manifold outlet and at 0.25m, the light-off temperatures are possible as 80 s and 79 s, respectively.

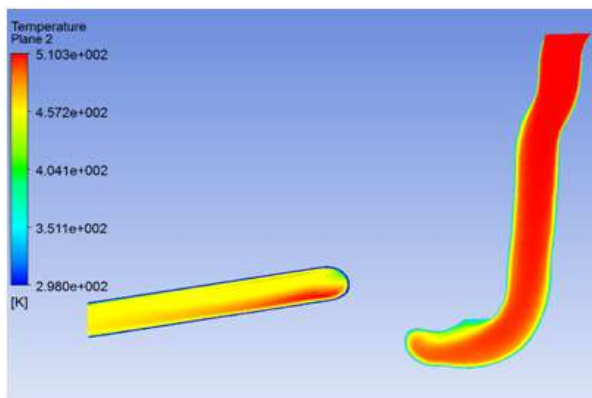


Figure 8. Variation of temperature on a plane at 123s.

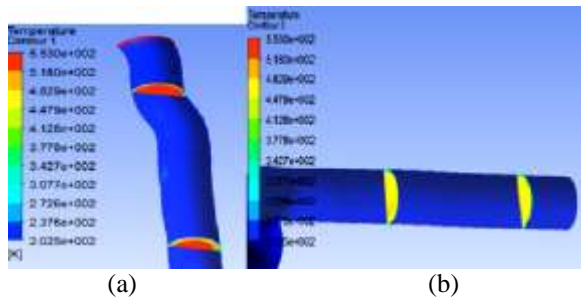


Figure 9. Temperature contours on different plane of inlet pipe (a) and outlet pipe (b) at 120s

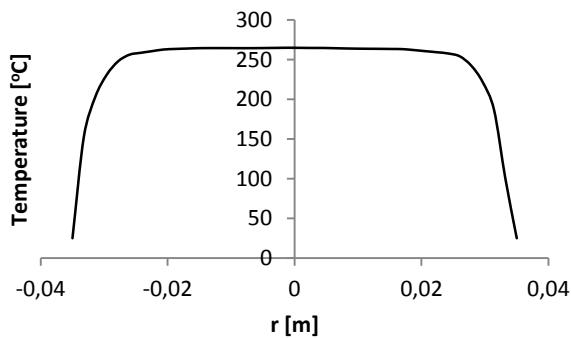


Figure 10. Temperature profile on a line of inlet pipe at  $y = 0.16$  m at 120s

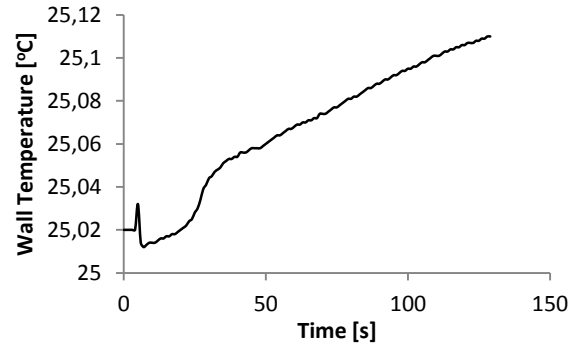


Figure 11. Wall temperature for inside wall of the exhaust pipe

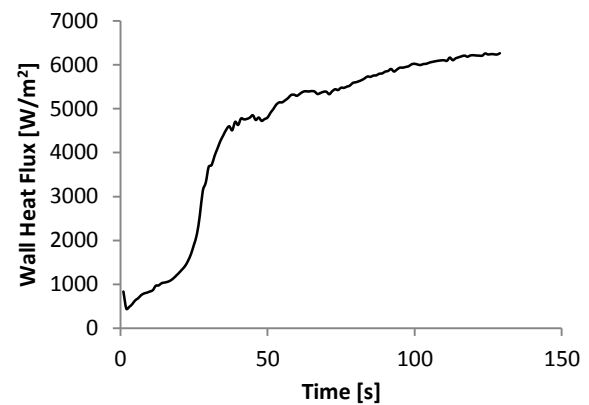


Figure 12. Wall heat flux for inside wall of the exhaust pipe

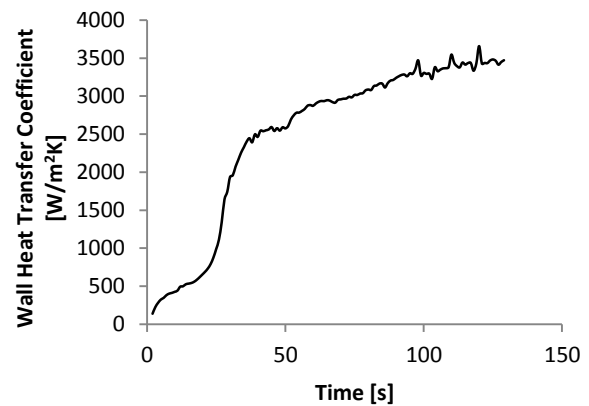
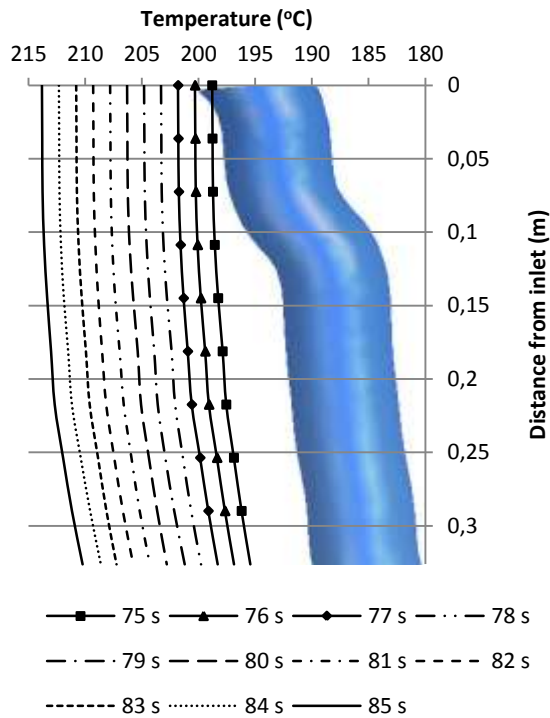


Figure 13. Wall heat transfer coefficient for inside wall of the exhaust pipe

### Results of Heat Transfer Analysis

Nusselt numbers obtained from equations 17 to 29 versus Reynolds number are compared to those of experimental data in Fig 15. Nusselt numbers calculated by Eq. 17 in range of  $9.4 \cdot 10^3 < Re < 12 \cdot 10^3$  using experimental data are compared to its values calculated by some correlations in literature (Figure 15). It is observed that the experimental Nusselt numbers behave near-linearly with increasing Re numbers. Equation of Meisner and Soreson (Eq. 23) gives significantly compatible with experimental data. It was observed that Gnielinski equation (Eq. 21) gave significantly lower





**Figure 14.** Temperatures on a line of center of inlet section of the exhaust pipe for various times

values than experimental data. CFD data agree especially with experimental data in higher Reynolds number. Equations of Shayler (Eq. 26) and Depcik and Assanis (Eq. 29) gives at close value to experimental data. Consequently, experimental results fit in with data which was reported in literature and showed an expected behavior.

## CONCLUSION

The design of the exhaust system of a spark ignition engine was thermally analyzed. An experimental study was carried out to compare the CFD and heat transfer analysis of gas flow in the exhaust pipe. In the experiments, the temperatures at inlet and outlet of the exhaust pipe were measured. CFD analysis was performed as three dimensional and transient regime. Density, specific heat capacity, thermal conductivity and dynamic viscosity of the exhaust gas were specified as functions of temperature by CCL expression in ANSYS CFX. Experimental values of the boundary conditions, which are mass flow rate and temperature at inlet and static pressure at outlet, were set in ANSYS CFX. Also the study aimed to investigate the heat transfer phenomena to get a better understanding analytically along with CFD analysis. The heat transfer coefficients varied in time were obtained by evaluating the experimental data. Experimental Nusselt number values were compared to available correlations obtained by the literature. The results showed that CFD provides a satisfactory estimation of fluid flow in the exhaust pipe. The heat transfer analysis showed that only one Nusselt number correlation could not describe the whole period of the heat transfer behaviors of the exhaust systems.

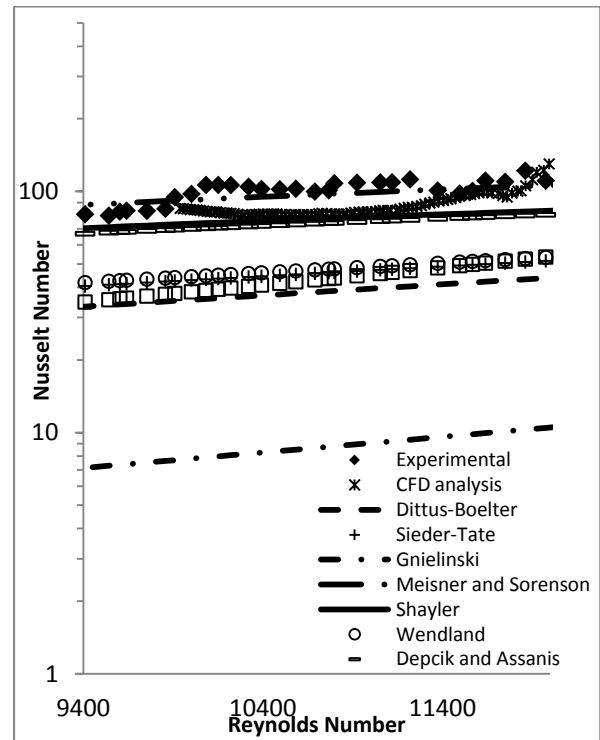


**Figure 15.** Comparisons Nusselt numbers.

The experimental results showed that the catalyst reached to the light-off temperature after 130 s at outlet of the exhaust pipe. The optimal catalyst location was obtained by CFD analysis in order to short necessary time to start the catalyst. If the catalyst was located closer than about 0.23 m to the manifold outlet, thus the catalytic converter would reach the light-off temperature at 77s.

The model presented in the study could be used for the determination of optimal location of a catalyst along with the exhaust pipe of any gasoline engine in terms of minimum cold start HC emissions. In addition, the model can be used for any type motor with exhaust system requiring HC emissions.

## REFERENCES

- Abarhama M., Hoarda J.W., Assanisa D., Stylesb D., Scott Sluderc C.S., Storeyc J.M.E, 2010, An Analytical Study of Thermophoretic Particulate Deposition in Turbulent Pipe Flows, *Aerosol Science and Technology*, 44-9, 785-795.
- ANSYS, 2009, *Turbulence, Introduction to CFX* , ANSYS Training Manual, Chapter 9.
- ANSYS, 2010, *Solver Theory Guide*, ANSYS CFX Release 12.1 Manual.
- Baba N., Ohsawa K., and Sugiura S., 1996, Numerical Approach for Improving the Conversion Characteristics of Exhaust Catalysts Under Warming-Up Condition, *SAE Technical Paper*, 962076, doi:10.4271/962076.

- Bagheri N., White B.R., Lin W., and Ayala A., 1995, Adverse-Pressure-Gradient Thermal Structure For Constant Wall Temperature Turbulent Boundary Layer, *33rd Aerospace Sciences Meeting and Exhibit*, Reno, NV, 95- 0022.
- Bardina J.E., Huang P.G., Coakley T.J., 1997, Turbulence Modeling Validation, Testing, and Development, *NASA Technical Memorandum*, 110446.
- Boam D., Clark T., and Hobbs K., 1995, The Influence of Fuel Management on Unburnt Hydrocarbon Emissions During the ECE 15 and US FTP Drive Cycles, *SAE Technical Paper*, 950930, doi:10.4271/950930.
- Buznik V.M., Artemov G.A., Bandura V.N., Fedorovskii A. M., 1966, Heat transfer on a plate in a turbulent flow with constant surface heat flux and an isothermal wall, *Journal of Engineering Physics and Thermophysics*, 11-1, 68-69, DOI: 10.1007/BF00829936.
- Caton J.A., Heywood J.B., 1981, An experimental and analytical study of heat transfer in an engine exhaust port, *International Journal of Heat and Mass Transfer*, 24 (4), 581–595.
- Chan S.H., Hoang D.L., 1999, Heat transfer and chemical reactions in exhaust system of a cold-start engine, *International Journal of Heat and Mass Transfer*, 42, 4165-4183.
- Depcik C. and Assanis D., 2002, A Universal Heat Transfer Correlation for Intake and Exhaust Flows in an Spark-Ignition Internal Combustion Engine, *SAE Technical Paper*, 2002-01-0372, doi:10.4271/2002-01-0372.
- Favez J.Y., Weilenmann M., Stilli J., 2009, Cold start extra emissions as a function of engine stop time: Evolution over the last 10 years, *Atmospheric Environment*, 43, 996–1007.
- Galloopoulos N., 1992, Bridging the Present to the Future in Personal Transportation - The Role of Internal Combustion Engines, *SAE Technical Paper*, 920721, doi:10.4271/920721.
- Hattori F., Takeda K., Yaegashi T., Harada A., 1997, Analysis of fuel and combustion behavior during cold starting SI gasoline engine, *JSAE Review*, 18, 351-359.
- Henein N.A., Tagomori M.K., 1999, Cold-start hydrocarbon emissions in port-injected gasoline engines, *Progress in Energy and Combustion Science*, 25, 563–593.
- Hua L., Yingjie Z., Xuemei Z., Kai D., Haihao L., Luyin C., 2007, Experimental Study of Convective Heat Transfer in Pulsating Air Flow inside Circular Pipe, *Challenges of Power Engineering and Environment*, 10, 880-885.
- Kandylas I.P., Stamatelos A.M., 1999, B Engine exhaust system design based on heat transfer computation, *Energy Conversion & Management*, 40, 1057-1072.
- Koltsakis G.C., Konstantinidis P.A., Stamatelos, A.M., 1997, Development and application range of mathematical models for 3-way catalytic converters, *Applied Catalysis B: Environmental*, 12, 161-191.
- Marineau E.C., Schetz J.A., Neel R.E., 2007, Turbulent Navier-Stokes Simulations of Heat Transfer with Complex Wall Temperature Variations, *Journal of Thermophysics and Heat Transfer*, 21-3, 525-535.
- Meisner S. and Sorenson S., 1986, Computer Simulation of Intake and Exhaust Manifold Flow and Heat Transfer, *SAE Technical Paper*, 860242, doi:10.4271/860242.
- Petukhov B.S., 1970, Heat transfer and friction in turbulent pipe flow with variable physical properties, *Advances in Heat Transfer*, 6, 503-565.
- Pinelli M., Bucci G., 2009, Numerical based design of exhaust gas system in a cogeneration power plant, *Applied Energy*, 86, 857–866.
- Sachdev R.; Sorenson S.C., 1981, An Investigation of Instantaneous Heat Transfer Rates in the Exhaust Port of an Internal Combustion Engine, *U.S. Army Research Office*, DAAG2978G0133, DAAG2976G0265.
- Shayler P.J., Harb C., Ma T., 1995, Time Dependent Behaviour of Heat Transfer Coefficients for Exhaust Systems, *IMEchE Paper C496/046/95, Proc VTMS2 Conference*, London, 195-206.
- Silva C.M., Costa M., Farias T.L., Santos H., 2006, Evaluation of SI engine exhaust gas emissions upstream and downstream of the catalytic converter, *Energy Conversion and Management*, 47, 2811–2828
- Sorin A., Bouloc F., Bourouga B., Anthoine P., 2008, Experimental study of periodic heat transfer coefficient in the entrance zone of an exhaust pipe, *International Journal of Thermal Sciences*, 47, 1665–1675.
- Wendland D., 1993, Automobile Exhaust-System Steady-State Heat Transfer, *SAE Technical Paper*, 931085, doi:10.4271/931085.
- Yaegashi T., Yoshizaki K., Nagami T., Sugiura, S., Yoshinaga, T., Ohsawa, K., 1994, New Technology for Reducing the Power Consumption of Electrically Heated Catalysts, *SAE Technical Paper*, 940464, doi:10.4271/940464.



**Mesut DURAT** obtained his BS and MS Degrees in Machine Education from Sakarya University (Turkey) in 1995 and 2008, respectively. His doctorate in Machine Education from Sakarya University (Turkey) in 2006. He is now Assistant Professor at Sakarya University, with research interests on permanent mold casting, computer aided design, computer aided manufacturing and finite element design (thermal and structure).



**Zekeriya PARLAK** obtained his BS and MS Degrees in Mechanical Engineering from Trakya University and Sakarya University (Turkey) in 1998 and 2004, respectively, and his Doctorate in Mechanical Engineering from Sakarya University (Turkey) in 2010. He is now Assistant Professor at Sakarya University, with research interests on thermal engineering optimization, thermal and fluid flow considerations in process engineering, Newtonian and non-Newtonian fluid flows in magnetorheological fluid flow considerations and magnetorheological devices.



**Murat KAPSIZ** obtained his BS and MS Degrees in Machine Education from Sakarya University (Turkey) in 2001 and 2004, respectively. He is now Research Assistant at Sakarya University, with research interests on internal combustion engine, Tribology, Alternatives Energy and coatings technology.



**Adnan PARLAK** obtained his BS and MS Degrees in Marine Engineering Operations from İstanbul Technical University and Mechanical Engineering from Sakarya University (Turkey) in 1988 and 1996, respectively, and his Doctorate in Machine Education from Sakarya University (Turkey) in 2000. He is now Professor at Yildiz Technical University, with research interests on Marine engines, ceramic coating on engines, internal combustion engine.



**Ferit FIÇICI** obtained his BS and MS Degrees in Machine Education from Sakarya University (Turkey) in 2004 and 2006, respectively. He studying department of Renewable Energy Sources in Gebze Institute of Technology as specialist in 2005 and 2008, respectively. He is now Research Assistant at Sakarya University, with research interests on tribology, composites, computer aided design, computer aided manufacturing and finite element design (thermal and structure).